



Journal of Applied and Computational Mechanics



Research Paper

Proportional Topology Optimization under Reliability-based Constraints

Rodrigo Reis Amaral¹, Julian Alves Borges², Herbert Martins Gomes³

¹ Graduate Program in Mechanical Engineering, Federal University of Rio Grande do Sul,
Av. Sarmiento Leite, 425, Sala 202, 2^o Andar, 90050-170, Porto Alegre, RS, Brazil, Email: rodrigo_amaral_23@hotmail.com

² Graduate Program in Civil Engineering, Federal University of Rio Grande do Sul, Av. Osvaldo Aranha, 99, 3^o Andar, 90035-190, Porto Alegre, RS, Brazil, Email: jlnab@hotmail.com

³ Graduate Program in Mechanical Engineering, Federal University of Rio Grande do Sul,
Av. Sarmiento Leite, 425, Sala 202, 2^o Andar, 90050-170, Porto Alegre, RS, Brazil, Email: herbert@mecanica.ufrgs.br

Received September 02 2021; Revised October 10 2021; Accepted for publication November 04 2021.

Corresponding author: R.R. Amaral (rodrigo_amaral_23@hotmail.com)

© 2022 Published by Shahid Chamran University of Ahvaz

Abstract. Topology optimization is a methodology widely used in the design phase that has gained space in engineering. On the other hand, uncertainty is present in material properties, loads, and boundary conditions in practically any design. The main goal for this paper lies in the coupling of the two subjects to account for uncertainties in the topology optimization. The Proportional Topology Optimization method renders the possibility of treating the stress constraints in a unified way. This allows topologies that at the same time preserve structural reliability and optimize costs. The Proportional Topology Optimization method under the reliability constraint is presented for isostatic and hyperstatic beam examples with stress and displacement LSF.

Keywords: PTO; reliability analysis; uncertainty analysis; reliability-based topology optimization.

1. Introduction

In recent years, optimization methodologies have used metaheuristic algorithms to develop new structural solutions for mechanical problems. The purpose of improving an optimization process is to find the best and most suitable solutions (materials properties and sizes) for the structures as long as they are feasible and the overall objective is achievable in practice (Bekdas et al. [1]).

According to Kongwat and Hasegawa [2], structural optimization is classified into three types: sizing optimization, shape optimization, and topological optimization. In sizing optimization, the structure is designed by adjusting the thickness/areas of each member within the structural design space. The geometry layout may not be preserved in shape optimization, like when the number of voids is maintained, but their dimensions are not. In topology optimization, the internal layout may freely vary. It starts with a defined design domain, and an ideal layout is achieved by redistributing and allocating the material. In other words, topological optimization is a computational process in which a surface or a volume of a structure, subjected to loads and boundaries conditions, changes its shape within that domain by allocating the material to attain some objective. Usually, the discretization of the computational domain is performed by the Finite Element Method. In this process, all finite elements become design variables of the problem due to a value they receive, called density. The attributed value for the design variables changes along with iterations (as densities). It is redistributed according to the pre-established objectives, for instance, maximizing stiffness, maximizing structural strength, maximizing dynamic behavior, etc., without disregarding constraints like the mechanical strength of the material.

In most studies that address topology optimization (Wang et al. [3], Zhang et al. [4], and Zhang and Yanagimoto [5]), the used design variables are treated as deterministic. In actual engineering problems, the exact values of many parameters can be unknown or have uncertainties since they cannot be measured accurately or even controlled. A deterministic topology optimization approach can lead to a sub-optimal or non-optimal actual design by neglecting the natural uncertainty present in the material's manufacturing process or even in the system's operating conditions (Gan and Wang [6]; da Silva et al. [7]).

The uncertainties of the stochastic variables can be considered in the topologic optimization by replacing the uncertain quantities with their higher-order statistics. This is performed in Robust Design Optimization (RDO) and Reliability-based Design Optimization (RBDO). For the RDO case, the objective is to minimize uncertainties, such as variance in the cost and constraint functions. Typically, statistical moments for objective function and constraints are obtained by Monte Carlo Simulation or perturbation techniques that use Taylor series expansions. In RBDO, constraints are imposed on the probability of failure for expected performance. These constraints are usually approximated, like in First Order Reliability Method (FORM, Hasofer and Lind [8]) or Second-Order Reliability Method (SORM, Breitung [9]) that are based on first-order or second-order Taylor series expansions, respectively, of the performance functions (Ang and Tang [10]).



A novel algorithm to deal with robust topology optimization (RTO) under material and loading uncertainties is proposed in Rostami et al. [11]. As the first paper to use XFEM formulation in robust topology optimization, they use a truncated Gaussian random field for the random uncertainty analysis of the material property and load angle distribution. The robust optimization takes into account the mean value and standard variation of the compliance. Still, it considers neither the distribution type nor reliability index (failure probability), differentiating RTO problems from RBDO problems.

In this paper, reliability analyses with the displacement and stress limit state functions (LSF) based on FORM to quantify the uncertainties and determine the new optimized topologies by the Proportional Topology Optimization (PTO) method are presented. The novelty relies on the framework of including the RBDO in the topology optimization in a double loop scheme. The reliability analysis is an inner loop of the Topology optimization outer loop. Beams are analyzed with the PTO method (based on the Bidirectional Evolutionary Structural Optimization, BESO). The reason for adopting the PTO method is that the formulation allows the designer to develop topologies without providing a constraint volume or evaluating an objective function gradient. Besides, a PTO algorithm generally yields topologies with lower stresses than topologies obtained by traditional compliance-based algorithms (Biyikli and To [12]). In addition, it has been proven the equivalence in strain energy and stress criterion-based approaches in terms of obtained final topology and compliance, with the advantage the second deals directly with stress constraints (Li et al. [13]). Furthermore, a sensitivity analysis is carried out to assist in the design decisions of topologically optimized structures, revealing the uncertain variables' relative importance in the final reliability. The failure probability and the corresponding reliability index β of optimized geometries are obtained in numerical examples for a simply supported beam and a double-clamped beam. The results show the importance of taking into account this reliability constraint in the final topology to assure a safe and cost-effective design.

The paper is organized as follows: a brief literature review on topology optimization that considers uncertainties is performed. Then, the basis for the Proportional Topology Optimization is presented, followed by the main concepts and algorithm used for reliability analysis. Lastly, two numerical examples are presented regarding the use of the proposed methodology.

2. Literature Review

Among the works that address topological optimization with uncertainties in the material variables, design variables, or applied load, Kharmanda et al. [14] proposed a new methodology to integrate reliability constraints into a topology optimization problem. The study demonstrated that structures optimized with these new constraints were more reliable than those obtained by deterministic optimization. Besides, the study made it possible to generate different topologies under different reliability levels with this new approach.

Jung and Cho [15] presented the topology optimization of three-dimensional Mindlin plate structures using the RBDO framework. For the reliable topology design, uncertainties of the material property and the external loads were considered. The numerical examples for the topology design show that the RBDO could handle the design uncertainty more effectively than any other approach, such as the safety factor and the worst-case approaches.

Tootkaboni et al. [16] presented a robust topology optimization algorithm for continuum structures in the presence of uncertainties. The optimized process under constraints considered combinations of the mean and the standard deviation of structural response. Also, it was used a deterministic topology optimization method in combination with a spectral stochastic approach, based on Polynomial Chaos Expansion and Stochastic Galerkin methods to represent and quantify structural stiffness uncertainties. The results demonstrated that this new methodology is most appropriate for highly correlated uncertainties. Weakly correlated or uncorrelated random fields would require higher dimensional Polynomial Chaos Expansion.

Similarly, Ghasemi et al. [17] proposed an uncertainty propagation and use of metamodel to optimize composites with nanotubes (CNT) using stochastic multi-scale modeling. This study considered CNT waviness, agglomeration, applied load, and finite element discretization as random fields. Besides, a reliability constraint evaluated by the First Order method is applied, but no topology optimization is performed.

A methodology for topology optimization of multi-material-based of flexoelectric composites was proposed by Ghasemi et al. [18]. It adopted a deterministic multiphase vector level-set model, which copes with various phases, and efficiently satisfies multiple constraints. The numerical examples showed the capabilities of the model to design two, three, and four-phase micro-sensors with the optimal electromechanical coupling coefficient (ECC). They report the normalized ECC resulted 2.5 times larger than that obtained from a beam made purely from the active material.

An approach based on level-set topology optimization (another topology optimization method that incorporates an implicit representation of the boundary, commonly as a signed distance function) was presented by Guo et al. [19]. The uncertainty was present in the structural boundary conditions. To make the optimal designs less sensitive to the possible boundary variations, the compliance and fundamental frequency of structure enduring the worst-case perturbation as the objective function was chosen. The obtained optimal structure was found to have better robustness when it was compared to their deterministic counterparts.

Luo et al. [20] proposed an effective method for stress-constrained topology optimization problems under load and material uncertainties. This study demonstrated that the optimal topologies obtained by the proposed RBDO approach were distinctly different from the deterministic design, providing, in this way, initial guidance for a safer design. Besides, the simultaneous consideration of the ϵ -relaxation (Cheng and Guo [21]) and a new reduction strategy on the target reliability index have shown avoiding the singularity of reliability-based stress constraints.

A classical stress-based topology optimization problem considering uncertainties on Young's modulus by the RDO was described in da Silva and Cardoso [22]. The deterministic and the robust discretized optimization problems were solved using an augmented Lagrangian algorithm due to many stress constraints. It was shown that the structures obtained by the robust approach were heavier when compared to the deterministic ones.

António and Hoffbauer [23] proposed the RBDO of beam reinforced composite structures considering geometric nonlinear behavior. The proposed approach is a union of buckling and first-ply failure analysis of laminated reinforced beams. This study assumed the homogeneous orthotropic material mechanical properties of laminates as random, i.e., with uncertainties. The optimization could be addressed as a weight/cost minimization problem under safety constraints for buckling and first ply failure. The results demonstrated that the coefficients of variation of central point displacement and load factor have an asymptotic increase in the neighborhood of the buckling point.

A new method to incorporate constraints on the first-passage probability into topology reliability-based optimization of structural designs was proposed by Chun et al. [24]. This approach decouples a nested reliability analysis loop from the optimization loop by solving the sub-optimization problem based on simulation results. The numerical examples showed that the topology optimization framework could provide an efficient way for structural engineers to obtain cost-effective design solutions that satisfy probabilistic constraints on the stochastic response in the conceptual (and schematic) design process.

A generic framework for integrating Gaussian Processes with risk-based structural optimization was introduced by Keshavarzadeh et al. [25]. The work demonstrated robust and reliability-based design problems in the context of stress-based



topology optimization under imperfections in geometry, material properties, and loading variability. The study revealed that it is possible to approximate a non-trivial quantity such as maximum von Mises stress and its sensitivity based on parametric samples.

Contrarily, a non-probabilistic reliability-based topology optimization algorithm was proposed by Liu et al. [26]. Local material uncertainties were considering in additive manufacturing. The effects of local material uncertainties for the design of structures should embody the variation ranges of material properties and the spatial occurrence frequency of the extreme material properties. Comparing the results with deterministic designs, a more significant volume fraction is achieved to ensure a more reliable design due to the consideration of local extreme values due to material uncertainties.

Gomez et al. [27] proposed an efficient topology optimization framework for buildings subjected to stochastic ground motions based on SIMP (Solid Isotropic Material with Penalization). This study considered more realistic details in the topology optimization for aleatory excited buildings such as additional floor masses, additional gravity loads, diaphragm constraints, and models for ground motion. An envelope approach was adopted to deal with uncertainty and a newly adapted smooth objective and constraints functions. Interstory drifts were minimized using the braced systems obtained by topology optimization. The results demonstrated the efficiency of the proposed approach for topology optimization in buildings excited by ground motions, which offers a helpful tool for designers to explore new braced structural patterns for earthquake-prone areas.

3. Theoretical Basis

The optimization of a function, also known as a mathematical programming problem (in terms of minimization), can generally be written as follows (Rao [28]):

$$\begin{aligned}
 & \text{Find } \mathbf{Y} \{y_1, y_2, \dots, y_n\}^T, \text{ that minimizes } f(\mathbf{Y}) \\
 & \text{Subject to } g_i(\mathbf{Y}) \leq 0, \quad i = 1, \dots, m \quad \text{and} \quad l_j(\mathbf{Y}) = 0, \quad j = 1, \dots, p
 \end{aligned} \tag{1}$$

where \mathbf{Y} is called a vector of design variables, $f(\mathbf{Y})$ is the objective function, $g_i(\mathbf{Y})$ are the m inequality constraints, and $l_j(\mathbf{Y})$ are the p equality constraints. The existing and most adequate methods to solve this problem depend mainly on the types of design variables (integer, real, mixed), the difficulty in calculating gradients of the objective function, the number and types of constraints (and also the difficulty in their evaluation), and in the landscape of the objective function.

In this context, topological optimization is a methodology implemented in the Finite Element Method to better allocate material from a structure, under boundary and load conditions, to maximize or minimize predefined objective functions such as mass, natural frequencies, buckling load, etc. In this sense, it differs from parametric and shape optimization since the final structure can take any form within the original working space (volume).

3.1 Deterministic Proportional Topology Optimization

There are several approaches to address the topological optimization problem, such as Evolutionary Structural Optimization (ESO), Bidirectional Evolutionary Structural Optimization (BESO), Solid Isotropic Material Penalization (SIMP), Level-set, etc. For example, in the SIMP method (Bendsøe [29]), the domain is discretized into finite elements, and a density-based approach is used to represent the partial presence of material in the space region. Each finite element has an associated density y_e (design variables) that defines the stiffness of the element by its modulus of elasticity (isotropic material) $E_e = E_{min} + y_e^p (E_0 - E_{min})$ with $y_e \in [0,1]$, and a penalty factor p (ranging from 1 to 3), with E_0 and E_{min} being the material's modulus of elasticity and a minimum value to avoid total element removal, loss of mesh connectivity, and uniqueness of the inverse of the stiffness matrix. A fraction of the total volume of the structure $= vf \sum v_i$, where v_i is the volume of each element, and vf is the final volume fraction defined by the designer in the range [0,1] (usually treated as the constraint of the optimization problem).

In the BESO method, the associated densities y_e are discrete variables that can only assume values 0 or 1, or in a practical way y_{min} and 1, with y_{min} being a small value (in this work 1×10^{-3}). In stress optimization problems, to avoid singularity issues in the elemental stress calculation of elements that have been removed, in the context of BESO and SIMP, the concept of ϵ -relaxation is employed during the calculation process. In this way, it will relax the condition 0 and 1 for a state of intermediate densities (Le et al. [30]), returning to the condition of binary densities later. Thus, the topological optimization problem for minimum compliance (twice the elastic strain energy) with volume constraint can be posed as:

$$\begin{aligned}
 & \text{Minimize } \mathbf{C} = \mathbf{u}^T \mathbf{K} \mathbf{u} \\
 & \text{Subject to: } \sum y_i v_i - vf V_0 = 0, \quad \mathbf{K} \mathbf{u} = \mathbf{F}, \quad y_{min} \leq y_i \leq 1
 \end{aligned} \tag{2}$$

So, the obtained structure should comply with the minimum strain energy for the fixed final constraint volume, which can be seen as a material allocation problem.

Whereas the problem of topological optimization with stress constraint can be stated as:

$$\begin{aligned}
 & \text{Minimize } V = \sum_{i=1}^{n_{elem}} y_i v_i \\
 & \text{Subject to: } \mathbf{K} \mathbf{u} = \mathbf{F}, \quad \max(\sigma_i^{ym}) \leq \sigma_{lim}, \quad y_{min} \leq y_i \leq 1
 \end{aligned} \tag{3}$$

Problem (3), unlike (2), is non-convex and highly nonlinear (Biyikli and To [12]). It is noticed that in the second case, a target volume fraction is not defined. In this way, the value vf will no longer be a constraint of the problem but a result of the optimization once the process is finished and the stress constraint is met. The initial conditions of the problem (initial workspace, boundary conditions, and loads) must generate the structure that meets the stress constraint (from a feasible initial design) no matter the final volume attained. Obviously, in the second case, depending on σ_{lim} and external loads, there may be no solution.

In the context of BESO, $y_i = y_{min}$ or $y_i = 1$. The total volume of the target material (TM) to be reached in each iteration is given by $V_{i+1} = V_i(1 \pm ER)$, where ER is the evolutionary rate (percentage of material that will be removed or added at each iteration), and the signal will depend on whether the stress criterion is violated or not ($-$ if not violated and $+$ if violated). In the next step, the algorithm distributes the amount of target material V_{i+1} to the elements according to the stress ratio α_{is}^{norm} of each element or according to the sensitivity of each element α_{ic} . This explanation will be provided later. The target material must be distributed iteratively and weighted by the proportions of stress or by the strain energies. Then, solid elements ($y_i = 1$) that have a sensitivity lower than the limit sensitivity are removed from the design domain. Similarly, null elements ($y_i = y_{min}$) that have a sensitivity greater than the limit sensitivity are added to the design domain. The limit sensitivity is defined based on the total volume of the target material (TM). Here a density model for the elastic modulus of the material is used $E(y_i) = y_i^p E_1$, where E_1 denotes the



modulus of elasticity of a solid element and p penalizes the design variables in the direction of intermediate densities close to the x_{min} and close to 1 (extreme).

For a bi-dimensional isotropic linear structure, von Mises stresses are defined as:

$$\sigma_i^{vm} = \sqrt{\sigma_{xx}^2 - \sigma_{xx}\sigma_{yy} + \sigma_{yy}^2 + 3\tau_{xy}^2} \tag{4}$$

here $\sigma_i = (\sigma_{xx} \ \sigma_{yy} \ \tau_{xy})^T$ is the elemental stress tensor of element i in the vector form. In the Finite Element Analysis, the element stress can be evaluated from the displacement at nodes u_i , the constitutive matrix D , and the matrix that relates displacements and strains B for each finite element i , as $\sigma_i = DBu_i$. In the SIMP method, the stress constraint is approximated since the real stress constraint is defined as $\max(\sigma_i^{vm}) - \sigma_{lim} \leq 0$ that is a non-differentiable function. The q-norm, adopted in this study, for the sensitivity analysis, evaluate the stresses weights in the elements (with empirical exponent q) so that the constraint can be formulated in a smooth way as $[\sum_{i=1}^{nelem} (\sigma_i^{vm})^q]^{1/q} \leq \sigma_{lim}$.

When the density interpolation scheme is employed, the stress on an element i is calculated as $\sigma_i = y_i^p DBu_i$ (assuming that the stress is located at the geometric center of the element) which is applied to Equation (5) and result in $\sigma_i^{vm} = y_i^p \sigma_{i0}^{vm}$ where the index σ_{i0}^{vm} represents the von Mises stress in the solid element i ($y_i = 1$) and a weighting factor. The sensitivity of finite element stresses to design variables y_i is defined as:

$$\alpha_i = \frac{\sigma_i^{vm}}{y_i} = y_i^{p-1} \sigma_{i0}^{vm} \tag{5}$$

The sensitivity will indicate the preference for distribution (removal/addition) of elements in the finite element mesh. Obviously, for finite elements with $y_i = 1, \alpha_i = \sigma_{i0}^{vm}$ and for elements with $y_i = y_{min}, \alpha_i = y_{min}^{p-1} \sigma_{i0}^{vm}$ that for $p \gg 1$, it will result in $\alpha_i = 0$. This study uses the degree of a proportion of von Mises stress, following the definition given by Biyikli and To [12].

$$\alpha_i^{norm} = \frac{(\sigma_i^{vm})^q v_i}{\sum_{i=1}^{nelem} (\sigma_i^{vm})^q v_i} \tag{6}$$

where v_i is the volume of the finite element i , q is an exponent of proportionality, and $nelem$ is the number of elements in the structure.

Most of the literature works with a slightly different objective function from the degree of a proportion, the compliance, although the equivalence has been proven (Li et al. [9]). In this case, the objective function to be optimized is half the compliance, as defined according to Huang and Xie [31] as the total elastic strain energy of a structure or half the work done by the external forces:

$$C = \frac{1}{2} f^T u = \frac{1}{2} u^T K u \tag{7}$$

When a solid element is removed from the structure, the change in the total elastic strain energy is equal to the elastic strain energy of the removed element. Thus, the sensitivity for each finite element i can be defined as:

$$\alpha_i = \frac{1}{2} u_i^T K_i u_i \tag{8}$$

where u_i are the degrees of freedom associated with the finite element i , and K_i is the elemental stiffness for the element i . Equation (8) indicates that the decrease in compliance due to the removal of an element i is equal to the deformation energy of the element itself. This definition is called hard-kill BESO and is a particular case of the soft-kill BESO method, where the elastic strain energy of the element is not entirely removed but penalized. The soft-kill method incorporates a penalized material model for the elastic properties such that $E(y_i) = y_i^p E_1$, with y_i being the density of the finite element $i \in [y_{min} \ 1]$ and p is a penalization factor. Therefore, the sensitivity number that defines the relative ranking of an individual finite element to be removed or added is defined as:

$$\alpha_i = \frac{y_i^{p-1}}{2} u_i^T K_i^0 u_i \tag{9}$$

where K_i^0 is the stiffness matrix of the solid element, and p is a penalty factor. For $y_i = 1$, the above equation turns to the previous equation (8). Note that when p tends to infinity, the stiffness and sensitivity of elements with intermediate densities tend to zero, bringing design variable values closer to the extremes y_{min} and 1.

In topological optimization works, it is usual to use sensitivity filters to avoid edges in the final topology to prevent the phenomenon of the checkboard pattern and mesh dependency. A simple linear filter is used in this paper and can be defined as:

$$\alpha_i = \frac{\sum_{j=1}^N \omega(r_{ij}) \alpha_j^n}{\sum_{j=1}^N \omega(r_{ij})} \tag{10}$$

where N is the number of nodes that are neighbors (at a distance less than or equal to r_{min}) of element i , r_{ij} is the distance between the center of the element i and node j , $\omega(r_{ij})$ are linear weighting factors $\omega(r_{ij}) = r_{min} - r_{ij}$ for $dist(i, j) < r_{min}$ and $\omega_{ij} = 0$ or $dist(i, j) \geq r_{min}$ and α_j^n is the sensitivity of the nodes within the neighborhood radius r_{min} with center at the finite element i . Equation (10) is applied to the sensitivity values of each element, resulting in smoothed values as a function of the neighboring values of that element. The final optimized structure will present truss-like members that have size cross-sections that depend on r_{min} and on the user's defined volume fraction vf (in compliance optimization problems) or user's defined limit stress σ_{lim} (in stress limited optimization problems). The reference Huang and Xie [31] is suggested for the filter scheme explanation for the reader's interest.

The sensitivity values defined in the previous sections for compliance or proportional stress can be weighted with the values of previous iterations to stabilize the method, for instance, $(\alpha^{norm})_{k+1} = \gamma(\alpha^{norm})_k + (1 - \gamma)(\alpha^{norm})_{k+1}$, using the stress proportion or $(\alpha_c)_{k+1} = \gamma(\alpha_c)_k + (1 - \gamma)(\alpha_c)_{k+1}$ using the compliance, where $\alpha = \{\alpha_1, \dots, \alpha_i\}^T$ is the vector of sensitivity numbers, k is the iteration counter, and γ is a moment factor (usually 0.5).

3.2 Reliability Analysis

Uncertainty is always present in nature. Two main types of uncertainties can be categorized as aleatory and epistemic uncertainties. The first one is related to the natural randomness found in material properties, unpredictable loads, boundary



conditions, or the modeling phase. The second one, also known as systematic uncertainty, comes from the lack of knowledge on underlying fundamental or total ignorance of the system behavior, lack of measurement, or its inaccuracy. This uncertainty can be reduced, but the first cannot. Once defined the requirement for the design's performance, the project's failure can be defined as not attaining this expected performance (maybe due to randomness), not necessarily to the catastrophic failure of the structure. For the determination of the probabilistic characteristics, a performance function should be declared. This function, called Limit State Function (LSF) and exposed in Eq. (11), will indicate when some expected performance is violated.

$$G(\mathbf{X}, \mathbf{d}) = R - S \tag{11}$$

where \mathbf{X} is the vector of random variables, \mathbf{d} is the vector or deterministic parameters, R is the resistance variable, and S is the demand variable. A safety condition is defined as the state where the LSF is positive ($G(\mathbf{X}, \mathbf{d}) > 0$) otherwise, it is defined as the failure condition. ($G(\mathbf{X}, \mathbf{d}) < 0$). The probability that a failure condition is attained ($P_f(\mathbf{X}, \mathbf{d})$) is defined by:

$$P_f(\mathbf{X}, \mathbf{d}) = \int_{-\infty}^{\infty} \int_{-\infty}^{s \geq r} f_R(r) f_S(s) dr ds = \int_{-\infty}^{\infty} F_R(x) f_S(x) dx = P[G(\mathbf{X}, \mathbf{d}) \leq 0] \tag{12}$$

where $f_S(S)$ is the probability density function of the load, and $f_R(r)$ is the cumulative probability density function of the resistance (Ang and Tang [7]). The assumption that S exceeds R corresponds to the overlapping area between $f_S(S)$ and $f_R(r)$ (i.e., failure region), which represents the quantitative measure of failure probability. Figure 1 explains this.

In Figure 1, $k_S \sigma_S = S_N$ represents an increased value for load actions and $k_R \sigma_R = R_N$ is a reduced value for the resistance, which accounts for uncertainties. An outdated measure of reliability used to be defined as a safety factor $SF = R_N/S_N$, being values greater than 1.0 considered reliable designs. This measure has several drawbacks and has been discredited. Besides, the performance function cannot be written in a simple linear form. Equation (12) can rarely be applied, so numerical procedures are used to give an approximation of the failure probability, such as simulation-based methods (Monte Carlo simulations and their variants) or First- and Second-Order Reliability Methods (FORM and SORM). The simulation methods usually demand high computational costs despite the high accuracy they can provide.

On the other hand, First and Second-Order Methods takes advantage of the Most Probable Point (MPP) contribution to the hypervolume of the failure domain in Equation (12). Since this point is the closest one, in the uncorrelated standard space, from the origin to the LSF, it is obtained by solving the following optimization problem:

$$\beta = \min \sqrt{\mathbf{U}^T \mathbf{U}} = \|\mathbf{U}\| \quad \text{subject to } G(\mathbf{X}, \mathbf{d}) = 0 \tag{13}$$

where \mathbf{U} is the vector of uncorrelated standard variables (usually a probabilistic transformation of the actual random vector \mathbf{X} to an uncorrelated normalized Gaussian space, $\mathbf{U} = \mathbf{L}^{-1}(\mathbf{X} - \mu_{eq})$ where $\text{cov}(\mathbf{X}, \mathbf{X}) = \mathbf{L} \mathbf{L}^T$ and μ_{eq} is the equivalent vector of Gaussian mean values. For a particular random variable i , $\mu_{eq,i} = x_i - \sigma_{eq,i} \Phi^{-1}[F_{X_i}(x_i)]$ and $\sigma_{eq,i} = \varphi\{\Phi^{-1}[F_{X_i}(x_i)]\} / f_{X_i}(x_i)$, where F_{X_i} stands for cumulative distribution, f_{X_i} means probability density function, Φ^{-1} is the inverse cumulative normal distribution and φ is the standard probability density function).

3.3 First Order Reliability Method

Using an iterative method (Hasofer and Lind [8]), the iterative equation for the solution of the problem in Equation (13) is given by:

$$\mathbf{U}^{k+1} = \left[\frac{\frac{\partial G^T}{\partial \mathbf{U}})^k \mathbf{U}^k - \left(\frac{\partial G}{\partial \mathbf{U}} \right)^k}{\left(\frac{\partial G^T}{\partial \mathbf{U}} \right)^k \left(\frac{\partial G}{\partial \mathbf{U}} \right)^k} \right] \left(\frac{\partial G}{\partial \mathbf{U}} \right)^k \quad \text{and} \quad \beta^{k+1} = \sqrt{(\mathbf{U}^T)^{k+1} \mathbf{U}^{k+1}} \tag{14}$$

A stopping criterion for iterations may be formulated based on the convergence of \mathbf{U} , β , and $G(\mathbf{X}, \mathbf{d}) = 0$. The measure of importance (sensitivity) of each random variable to the reliability index β can be evaluated by:

$$\theta = - \frac{\left(\frac{\partial G^T}{\partial \mathbf{U}} \right)^k}{\sqrt{\left(\frac{\partial G^T}{\partial \mathbf{U}} \right)^k \left(\frac{\partial G}{\partial \mathbf{U}} \right)^k}} \tag{15}$$

Considering the main contribution for the Most Probable Point (MPP) to the failure probability, an approximate relation (for linear LSF) between Failure Probability and the reliability index uses the definition of the standard cumulative distribution function (Φ) and is given by:

$$P_f = \Phi(-\beta) = 1 - \Phi(\beta) \tag{16}$$

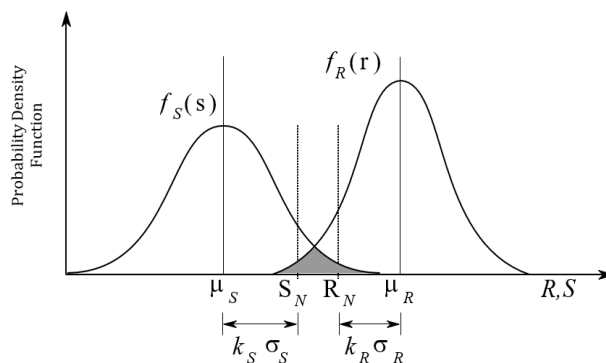


Fig. 1. The probability density function for load actions and resistance effects.



4. Numerical Examples

4.1 Reliability Analysis with Stress Limit State Function

The first example concerns the reliability of a simply supported beam subject to a vertical force applied at the midspan. The beam has a rectangular cross-section and is made of steel. A stress LSF is defined as $g(\mathbf{x}) = \sigma_{vM,lim} - \max(\sigma_{vM}(\mathbf{x}))$. Here, the max of the function assures that any point in the beam will be considered in the constraint equation. Six variables are chosen as random variables based on observed experimental variability and experimental data. The distribution type, mean values, and standard deviation for each of these random variables are: (i) yield strength based on the von Mises stress limit $\sigma_{vM,lim}(Pa)$ $N: (3 \times 10^8; 1.2 \times 10^7)$, (ii) the applied vertical load $F(N)$ $N: (4 \times 10^5; 4 \times 10^4)$, (iii) Modulus of Elasticity $E(Pa)$ $N: (2.1 \times 10^{11}; 2.1 \times 10^{10})$, (iv) beam's height $h(m)$, $N: (0.5; 0.025)$, (v) beam's width $t(m)$, $N: (0.15; 2.25 \times 10^{-3})$, and (vi) the beam's span $L(m)$, $N: (1; 0.01)$. The vector of random variables is defined as $\mathbf{x} = (\sigma_{vM,lim}, F, E, h, t, L)^T$. The Poisson coefficient, $\nu = 0.3$, is assumed deterministic because of the low coefficient of variation of this elastic property, as reported by Kuhinek et al. [32]. All the random variables are considered non-correlated. Besides, the Modulus of Elasticity and the yield strength limit are assumed constant within the finite element (evaluated at the element's center), and they take the same value in the whole design domain.

Four-node isoparametric finite elements are used to discretize the model with a structured mesh. The parameters adopted for the PTO method are: the final volume fraction $vf = 0.3$, the penalization for the proportional optimization $p = 3$, the number of elements in x direction $nelx = 200$, the number of elements in y direction $nely$ is obtained using the actual height h of the beam and the size of the mesh dx (half of the total length $L/2$ divided by $nelx$, since the finite elements have equal edges), the evolutive ratio is assumed as $ER = 0.05$ and $r_{min} = 3.5$ finite elements. It is adopted a moment factor of $\gamma = 0.5$ for stabilization of the topology optimization process. Since the LSF is based on local stresses, the applied load and the beam's support are equally applied over three adjacent nodes at the midspan to avoid stress concentration. Figure 2 shows the design domain and the adopted random variables.

Initially, a deterministic analysis is performed with the mean values of the random variables, and the final topology of the optimized structure and the corresponding compliance was evaluated. Figure 3 shows the final topology superimposed to the corresponding maximum von Mises stress and the values for compliance and maximum von Mises stress along with iterations. As expected, the maximum values occur near the point of application of the load and the beam's support (2.1534×10^8 Pa). The final compliance is $C = 142.0$ Nm. So, there is a Safety Factor for the yield strength of $SF = 1.39$.

The next step is to consider just one random variable, the von Mises yield stress limit ($\sigma_{vM,lim}$). This was meant to check the reliability evaluation steps since, in this case, the reliability can be easily evaluated in a closed-form: $P_f = \Phi\left(\frac{2.1534 \times 10^8 - 3.0 \times 10^8}{1.2 \times 10^7}\right) = 8.6300 \times 10^{-13}$. The corresponding reliability index is $\beta = -\Phi^{-1}(P_f) = 7.055$. When using the FORM method coupled with the finite element code, the obtained results are respectively, $P_f = 8.5588 \times 10^{-13}$ and $\beta = 7.0562$, which shows that the code for the reliability analysis and stress evaluation with finite elements is working well. The algorithm took 4 iteration steps to evaluate the reliability index and 8 LSF evaluations. Figure 4 shows the numerical results for this analysis.

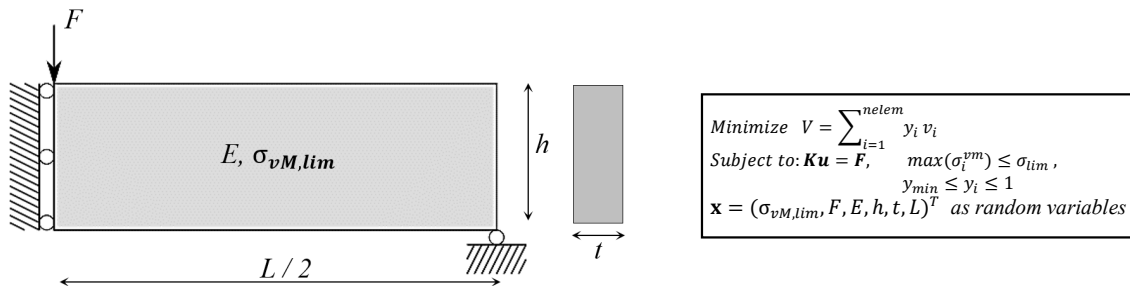


Fig. 2. Design domain for topology optimization and adopted random variables.

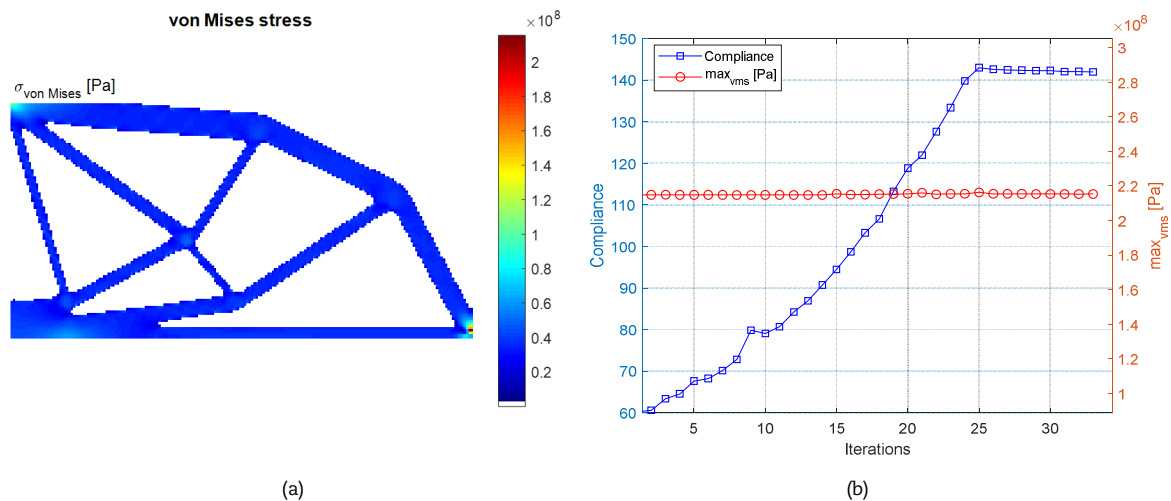


Fig. 3. (a) Final topology with von Mises stresses. (b) Compliance and maximum stress along with iterations.



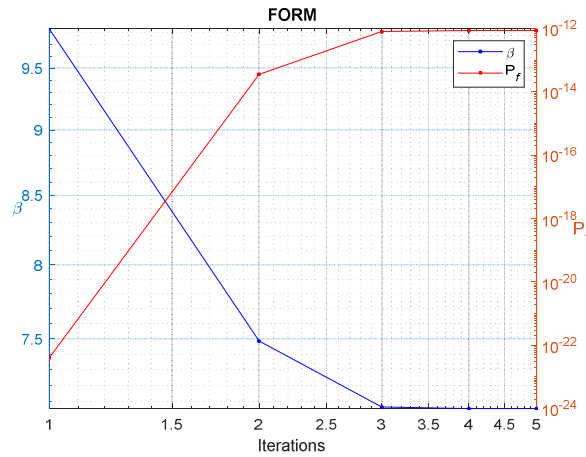


Fig. 4. Probability of Failure P_f and reliability index β convergence. Case of only yield stress limit as a random variable.

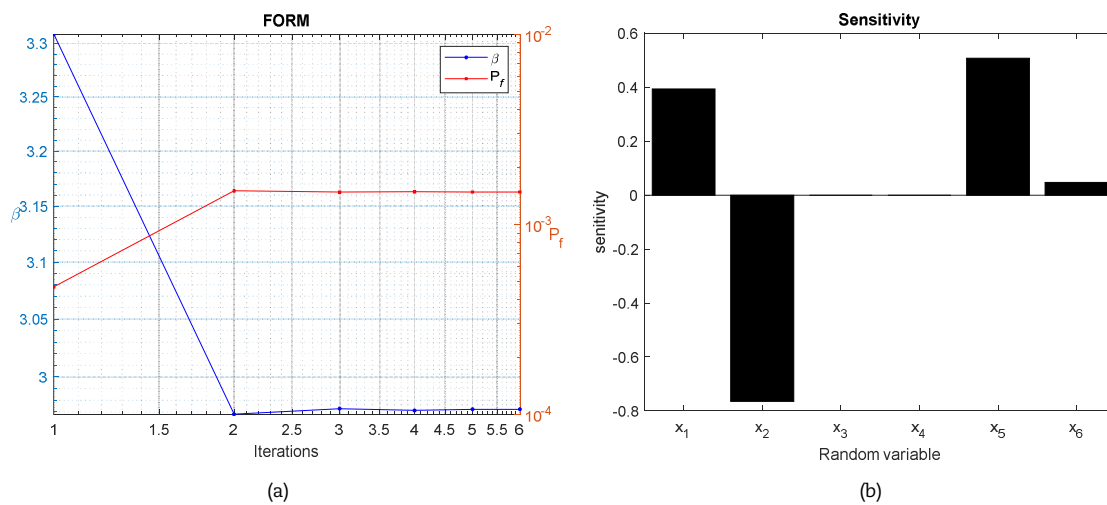


Fig. 5. Probability of Failure P_f and reliability index β convergence for six random variables case. (b) Sensitivity for each of the random variables.

The final step in this analysis is to consider more random variables. All six random variables are taken in the analysis. There is no closed-form solution for this case, so Figure 5 shows the numerical results obtained with the FORM algorithm coupled with the finite element code.

The results are respectively, $P_f = 1.4779 \times 10^{-3}$ and $\beta = 2.97$. The algorithm took 6 steps and 42 LSF evaluations. The load F (x_2 in Figure) presents the highest sensitivity to the reliability of the structure ($\theta_2 = -0.76$) among the random variables, followed by the beam's width t ($\theta_5 = 0.51$). The negative value of θ_2 means it inversely affects the reliability index. As expected for isostatic structures, like this simply supported beam, the modulus of elasticity does not affect the stresses, and so the structural reliability is $\theta_3 = 0$. The beam's height random variable h resulted in no sensitivity ($\theta_4 = 0$), which is not a common-sense result since height may influence bending stiffness and thus the maximum stress. This would be true in a regular full rectangular cross-section beam, but in the case of a topologically optimized structure, this seems to have no effect. In such structures, the stresses tend to uniformly distribute on the resulted truss-like members, decreasing the height influence on the reliability. The beam's length played a minor role ($\theta_6 = 0.05$), due to the low standard deviation for the length in this example.

4.2 Reliability-based Topology Optimization with Displacement Limit State Function

The second numerical example has the same material, design variables, random variables, boundary conditions and is exposed to a vertical load F as the previous example. However, in this case, a displacement LSF was considered. A maximum allowed displacement value of $w_{lim} = 6.60 \times 10^{-4} m$ was assumed. Besides, a target β will be adopted for this problem $\beta_{tgt} = 3.1$, as suggested by ISO 2394:2015 standard. Thus, making the volume fraction no longer a constraint of the problem, but a natural result from the reliability constraint, i.e., the situation becomes a Reliability-Based Topology Optimization (RBTO). It should be in mind that for a simply supported beam and small variations in the beam section and loads, the optimized structure will present maximum stress values very close to those from a non-optimized structure. This is the reason the LSF in this example is chosen to be mid-span displacement.

The results of these simulations are presented in Fig. 6. In this case, the final topology resulted in 59.26% of the initial material volume, and it took 11 iterations to converge, as can be observed in Fig. 6 (b). Regarding maximum displacements and structural strength, the optimized topology demonstrated a maximum displacement w_{max} of $4.0755 \times 10^{-4} m$, a maximum von Mises stress $\sigma_{vM,max}$ of $2.1486 \times 10^8 Pa$. A final value of Compliance $C = 80.88 Nm$ was attained. So, there is a Safety Factor for the maximum structural displacements of $SF = 1.61$, and in the case of the material strength, $SF = 1.39$.



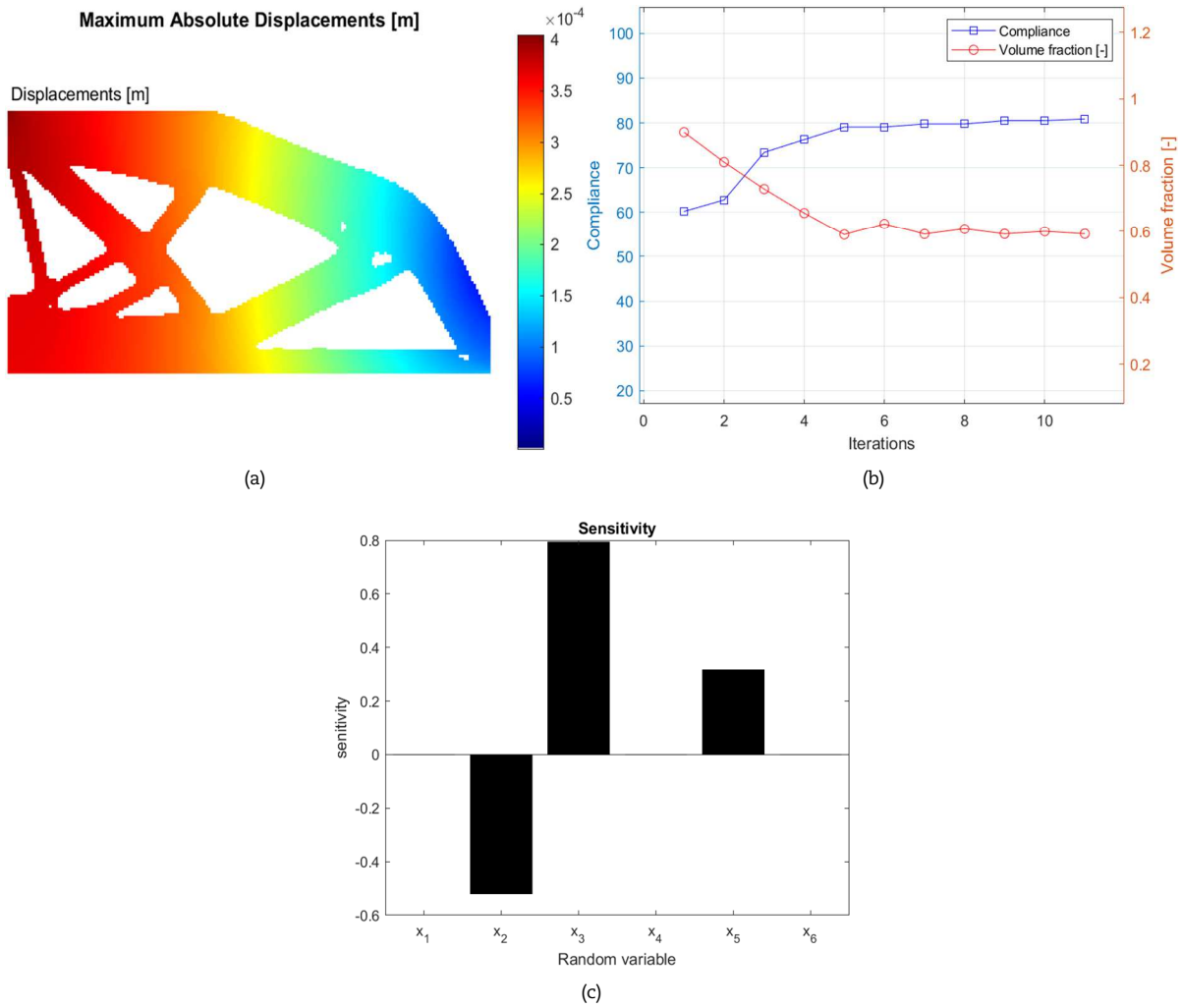


Fig. 6. (a) Final topology in deflected form. (b) Compliance and volumetric fraction along with iterations. (c) Sensitivity for each of the random variables.

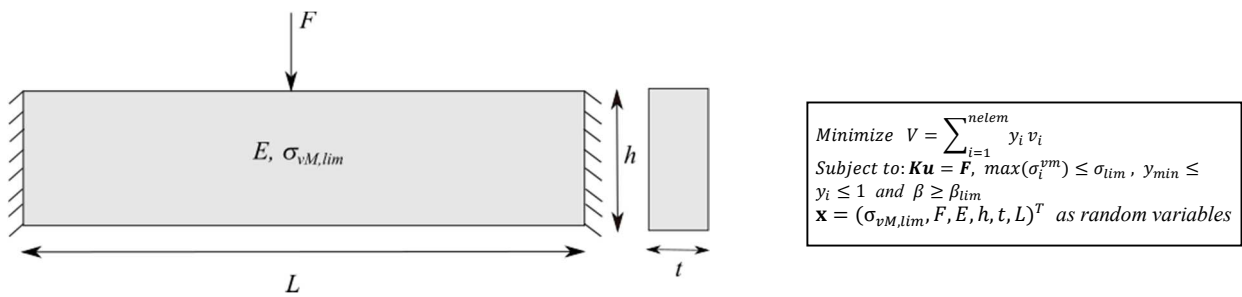


Fig. 7. Design domain for topology optimization of a double-clamped beam.

The final topology using the displacement LSF resulted in $\beta = 3.05$ and $P_f = 1.1630 \times 10^{-3}$. The stochastic variable that presents the higher sensitivity in this analysis is the modulus of elasticity E (x_3 in Figure 6(c)) with $\theta_3 = 0.79$, followed by the load F (x_2 in Figure 6(c)) with $\theta_2 = -0.52$. Unlike the previous analysis on stress LSF with only material strength as a random variable, in this example, the modulus of elasticity E presented a more significant sensitivity to the reliability because it is directly related to structural displacement.

4.3 Reliability-based Topology Optimization with Stress Limit State Function

The last example concerns an RBTO with the stress LSF of a double-clamped beam subjected to a vertical force applied at the midspan (Fig. 7). This example was intentionally modified from the previous one because this structure is more susceptible to maximum stress variations due to topology optimization. In this problem, the distribution type, mean values, and standard deviation for each of these random variables are: (i) yield strength based on the von Mises stress limit $\sigma_{vM,lim}$ (Pa) $N: (3 \times 10^8; 1.2 \times 10^7)$, (ii) the reference applied vertical load F_R (N) $N: (6 \times 10^5; 6 \times 10^4)$, (iii) Modulus of Elasticity E (Pa) $N: (2.1 \times 10^{11}; 2.1 \times 10^{10})$, (iv) beam's height h (m) $N: (0.3; 0.015)$, (v) beam's width t (m) $N: (0.20; 0.01)$, and (vi) the beam's span L (m) $N: (3; 0.015)$. So, the vector of random variables is defined as $\mathbf{x} = (\sigma_{vM,lim}, F, E, h, t, L)^T$. The Poisson coefficient $\nu = 0.3$ is assumed deterministic, as the first and previous example, and all the random variables are considered non-correlated. The parameters adopted for the PTO method are the same adopted in the previous examples. Again, the volume fraction is not a constraint of the optimization problem since the reliability index for stress will rule the final volume fraction and is the criterion for stopping the topology optimization.



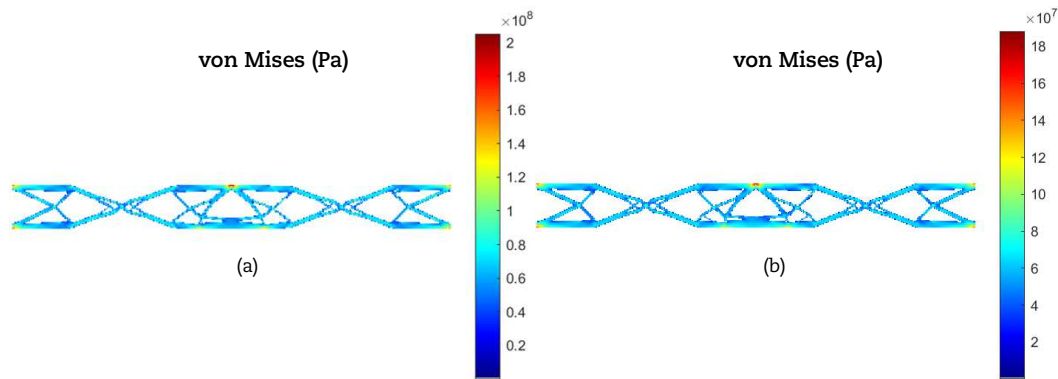


Fig. 8. Final topology for a target reliability index for structural elements of agricultural buildings with a reference life span of (a) 50 years ($\beta = 3.37$) and (b) 1 year ($\beta = 4.28$).

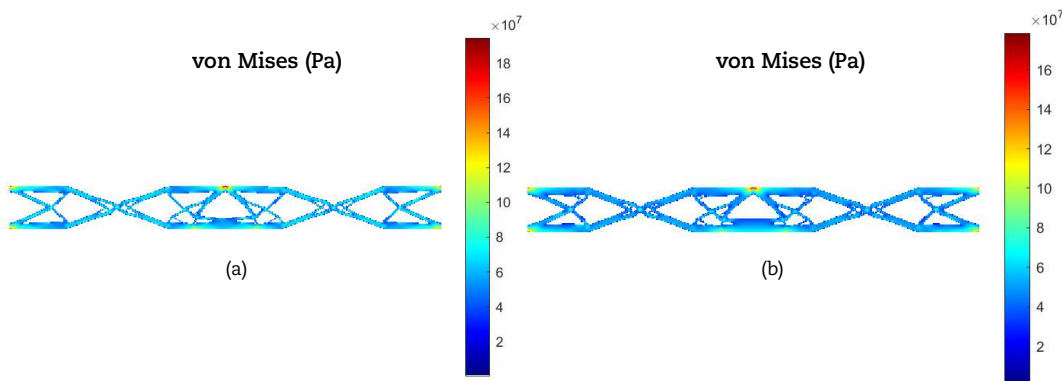


Fig. 9. Final topology for a target reliability index for structural elements of residential buildings with a reference life span of (a) 50 years ($\beta = 3.86$) and (b) 1 year ($\beta = 4.73$).

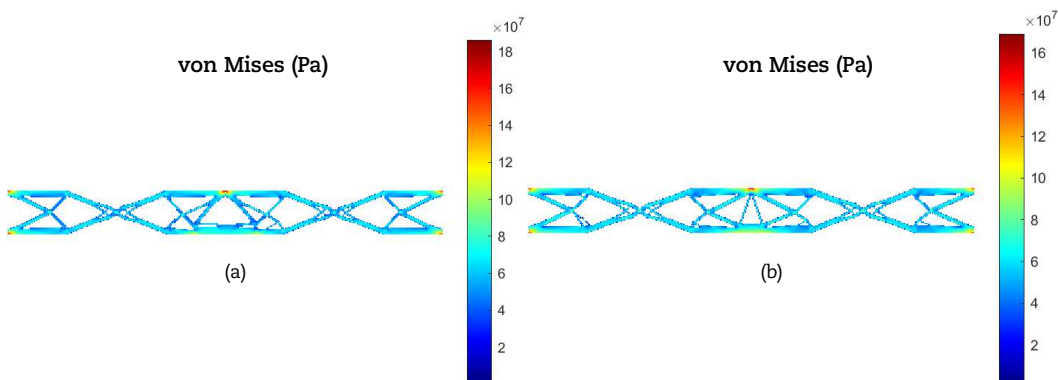


Fig. 10. Final topology for a target reliability index for structural elements of civil buildings with a reference life span of (a) 50 years ($\beta = 4.29$) and (b) 1 year ($\beta = 5.20$).

The first analysis performed in this section is optimizing this structure according to reliability target values from EN 1990. The recommended reliability index must be around $3.3 \leq \beta \leq 4.3$ for a reference service life of 50 years, and $4.2 \leq \beta \leq 5.2$ for a service life of 1 year, so that the lowest value refers to agricultural structural elements, the mean value for each interval (3.8 and 4.7) refers to residential structures and the highest value, to civil structures. These target reliability values will be used as reliability constraints for the topology optimization. The results are presented in Figs. 8, 9, and 10.

The structures with a reference life of 1 year presented a high level of safety due to the low value of the von Mises stress found in the simulations. That is, this value resulted in $169.19 \times 10^6 \leq \sigma_{vM} \leq 188.15 \times 10^6$ Pa. In addition, it was observed that for the reliability in structural elements for residential buildings, Fig. 9 (b) presented the heavier structure (higher volume fraction of retained material), the final topology resulted in 44.49% of volume fraction. The structure with the highest reliability index, Fig. 10 (b), resulting in 39.04% of volume fraction. Besides, it was noted that in the case of structural elements of residential buildings, the final structure presented a higher concentration of stress than the other solutions. This is explained by the cases $\beta = 4.29$ and $\beta = 5.20$ for showing a better stress distribution within the remaining material.

Regarding the structures with a reference service life of 50 years, the von Mises stress value found in the simulations varied from $186.19 \times 10^6 \leq \sigma_{vM} \leq 205.24 \times 10^6$ Pa, which represents a strength Safety Factor of $1.46 \leq SF \leq 1.61$. As occurred for the reference of 1-year service life, the intermediate reliability index, Fig. 9 (a), presented the heavier structure since the final topology resulted in 37.14% of volume fraction and the structure with the lowest reliability index, Fig. 8 (a), resulted in 34.18% of volume fraction (the topology that removed more material). Unlike the structures with a reference service life of 1 year, all the structures showed an excellent stress distribution throughout their remaining material. However, the locations where loads and supports were applied still show the highest concentration for stress states.



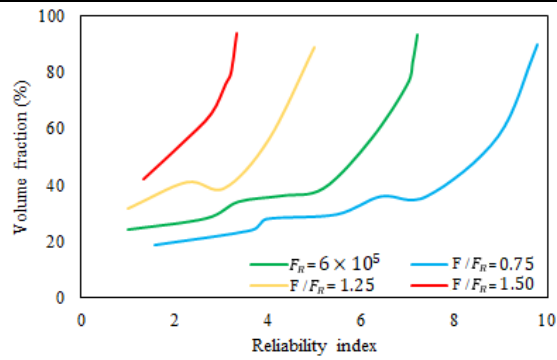


Fig. 11. Variation of reliability indexes β and the applied load.

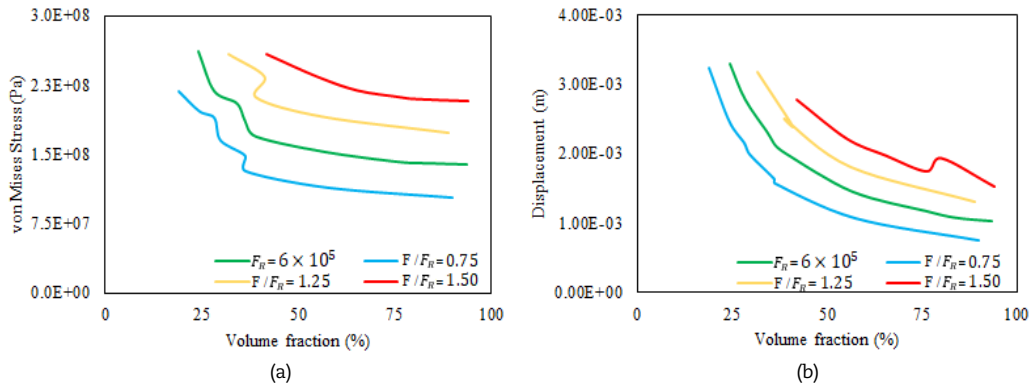


Fig. 12. Variation of: (a) von Mises stress and (b) displacement related to the retained material for an RBTO with stress LSF.

Finally, an analysis of the variation of the load on this structure will be developed. The objective here is to determine the minimum and maximum values of the reliability index β for each nominal load value adopted. For this, a reference load $F_R = 6 \times 10^5$ N will be used as the basis for the other loads considered, as seen in Fig. 11. Besides that, graphics were plotted relating the structural stiffness and strength of the structure to the volume fraction of retained material obtained with the RBDO with stress LSF (Fig 12 (a) and (b)).

In Fig. 11, for each F/F_R ratio, it was set increasing reliability indexes, and the corresponding final volume fraction was obtained. In the case of Fig. 12, the maximum von Mises stress and displacement for the same cases of Figure 11 are plotted against the final volume fraction.

The results in Fig. 11 indicate that the addressed problem can support a 25% higher load than the reference load F_R and even attain some of the required target reliability described in EN 1990. For example, if one considers a vertical load of $F = 7.5 \times 10^5$ N ($F/F_R = 1.25$), the reliability index of the topologically optimized double-clamped beam is around $1.0 \leq \beta \leq 5.0$ as indicated by Fig. 11, making it possible to assume that this structural element is complying with the target reliability for structural elements in agricultural and residential buildings. Furthermore, using topology optimization, it is feasible to remove 60.96% of the material for a reliability index of $\beta = 3.1$ and remove 11.07% for a reliability index of $\beta = 5.0$. Yet, for this case, it was observed that the von Mises stress varied from $173.94 \times 10^6 \leq \sigma_{vM} \leq 211.49 \times 10^6$ or 257.98×10^6 Pa (if EN 1990 is disregarded, resulting $\beta \leq 3.3$). For the maximum displacements, it varied from 3.1771×10^{-3} (if EN 1990 is disregarded) or $2.4976 \times 10^{-3} \leq w_{max} \leq 1.3053 \times 10^{-3}$ m (Fig. 12).

Concerning the load case $F = 9.0 \times 10^5$ N ($F/F_R = 1.50$), in Fig. 11, the reliability index of the double-clamped beam is about $1.35 \leq \beta \leq 3.3$, thus, making the problem unfeasible to the parameters required by EN 1990 standard. In the case of $F/F_R = 0.75$, the structural element has high reliability, which implies the possibility of retaining less material and obtaining a lighter structure.

5. Conclusions

This study presents numerical examples of topologically optimized beams by the PTO method when considering reliability analysis with uncertainty in material properties, applied load, and geometric parameters. Also, a sensitivity analysis of the variables is done to determine how much they affect the process of topology optimization with uncertainties using the FORM. In this way, the paper emphasizes the importance of considering uncertainties in the design phase, especially when taking into account the structural optimization process of the PTO (Proportional Topology Optimization) method (based on BESO).

The first example dealt with a reliability analysis of a simply supported beam when considering a stress LSF. The sensitivity analysis of the variables related to the material, applied load and the geometrical dimensions showed that for isostatic problems, the applied load has a more significant influence on the result, followed by the thickness considered for the beam.

Using the same numerical beam model but now considering a displacement LSF, the second example turned the problem into a Reliability-Based Topology Optimization (RBTO). In other words, a target reliability index β was stipulated as a constraint for the presented problem, and the volume fraction is no longer a constraint. So, the higher the β , the earlier the material removal process will be interrupted, giving a chance to truss-like members to remain in the final optimized structure. In addition, as occurred in the previous example, random variables' influence was evaluated, demonstrating a more significant effect of the modulus of elasticity because it is directly related to displacements.

For the last example, an RBTO analysis was performed in a double-clamped beam with a stress LSF. First, a qualitative assessment of topologies that met target reliability indexes prescribed in EN 1990 was presented. In this step, it is demonstrated that optimized topologies with reliability constraints show thicker and heavier structural elements than those topologically optimized deterministic beams. Moreover, it is proved that the final topologies better distribute the stress throughout the remaining



material. However, there are stress concentration points at the supports and the location of the applied load. The other analysis carried out in this example aimed to demonstrate the reliability indexes' limits when varying the applied load's nominal value and relate the stiffness and structural strength with the material volume fraction. Here, it was presented that the topologically optimized structures would support a load 25% higher than the load initially stipulated, respecting the target reliability indexes from EN 1990 in the case of structural members of agricultural and residential buildings.

Author Contributions

Rodrigo Reis Amaral initiated the project, developed the reliability-based topology optimization, and analyzed the results; Julian Alves Borges verified the code for the reliability analysis and stress evaluation with finite elements; Herbert Martins Gomes planned the scheme, developed the reliability Matlab code, analyzed the results and led the project. The manuscript was written through the contribution of all authors. All authors discussed the results, reviewed, and approved the final version of the manuscript.

Acknowledgments

This study was financed in part by the CAPES (Coordination for the Improvement of Higher Education Personnel) – Finance Code 001. The authors also thank CNPq (Brazilian National Council for Scientific and Technological Development).

Conflict of Interest

The authors declared no potential conflicts of interest concerning this article's research, authorship, and publication.

Funding

The authors received no financial support for this article's research, authorship, and publication.

Data Availability Statements

The datasets generated and/or analyzed during the current study are available from the corresponding author on reasonable request.


References


- [1] Bekdas, G., Nigdeli, S.M., Kayabekir, A.E., Yang, X., *Optimization in Civil Engineering and Metaheuristic Algorithms: A Review of State-of-the-Art Developments*, In: Computational Intelligence, Optimization and Inverse Problems with Applications in Engineering, 2019. https://doi.org/10.1007/978-3-319-96433-1_6.
- [2] Kongwat, S., Hasegawa H., Optimization on mechanical structure for material nonlinearity based on proportional topology method, *Journal of Advanced Simulation in Science and Engineering*, 6 (2), 2019, 354-366. <https://doi.org/10.15748/jasse.6.354>.
- [3] Wang, Y., Xu, H., Pasini, D., Multiscale isogeometric topology optimization for lattice materials, *Computer Methods in Applied Mechanics and Engineering*, 316, 2017, 568-585. <https://doi.org/10.1016/j.cma.2016.08.015>.
- [4] Zhang, J., Sato, Y., Yanagimoto, J., Homogenization-based topology optimization integrated with elastically isotropic lattices for additive manufacturing of ultralight and ultra-stiff structures, *CIRP Annals – Manufacturing Technology*, 70, 2021, 111-114. <https://doi.org/10.1016/j.cirp.2021.04.019>.
- [5] Zhang, J., Yanagimoto, J., Topology optimization of micro lattice dome with enhanced stiffness and energy absorption for additive manufacturing, *Composite Structures*, 255, 2021, 112889. <https://doi.org/10.1016/j.compstruct.2020.112889>.
- [6] Gan, N., Wang, Q., Topology optimization design of improved response surface method for time-variant reliability, *Advances in Engineering Software*, 146, 2020, 102828. <https://doi.org/10.1016/j.advengsoft.2020.102828>.
- [7] da Silva, G.A., Cardoso, E.L., Beck, A.T., Comparison of robust, reliability-based and non-probabilistic topology optimization under uncertain loads and stress constraints, *Probabilistic Engineering Mechanics*, 59, 2020, 103039. <https://doi.org/10.1016/j.probenmech.2020.103039>.
- [8] Hasofer, A.M., Lind, D., An exact and invariant first-order reliability format, *Journal of Engineering Mechanics*, 100, 1974, 111-121.
- [9] Breitung, K., Asymptotic Approximations for Multinomial Integrals, *Journal of Engineering Mechanics*, 110(3), 1984, 357-366.
- [10] Ang, A.H.S., Tang, W.H., *Probability Concepts in Engineering: Emphasis on Applications to Civil and Environmental Engineering*; Wiley; 2nd Edition, 2006.
- [11] Rostami, S. A. L., Kolahdooz, A., Zhang, J., Robust topology optimization under material and loading uncertainties using an evolutionary structural extended finite element method, *Engineering Analysis with Boundary Elements*, 133, 2021, 61-70. <https://doi.org/10.1016/j.enganabound.2021.08.023>.
- [12] Biyikli, E., To, A.C., Proportional Topology Optimization: A New Non-Sensitivity Method for Solving Stress Constrained and Minimum Compliance Problems and Its Implementation in MATLAB, *PLoS ONE*, 10(12), 2015. <https://doi.org/10.1371/journal.pone.0145041>.
- [13] Li, Q., Steven, G.P., Xie, Y. M., On the equivalence between stress criterion and stiffness criterion in evolutionary structural optimization, *Structural Optimization*, 18, 1999, 67-73.
- [14] Kharmanda, G., Olhoff, N., Mohamed, A., Lemaire, M., Reliability-based topology optimization, *Structural and Multidisciplinary Optimization*, 26, 2004, 295-307. <https://doi.org/10.1007/s00158-003-0322-7>.
- [15] Jung, H., Cho, S., Reliability-based topology optimization of geometrically nonlinear structures with loading and material uncertainties, *Finite Element in Analysis and Design*, 43, 2004, 311-331. <https://doi.org/10.1016/j.finel.2004.06.002>.
- [16] Tootkaboni, M., Asadbourne, A., Guest, J.K., Topology optimization of continuum structures under uncertainty – A polynomial Chaos approach, *Computer Methods in Applied Mechanics and Engineering*, 201-204, 2012, 263-276. <https://doi.org/10.1016/j.cma.2011.09.009>.
- [17] Ghasemi, H., Rañee, R., Zhuang, X., Muthu, J., Rabczuk, T., Uncertainties propagation in metamodel-based probabilistic optimization of CNT/polymer composite structure using stochastic multi-scale modeling, *Computational Materials Science*, 85, 2014, 295-305. <http://dx.doi.org/10.1016/j.commatsci.2014.01.020>.
- [18] Ghasemi, H., Park, H. S., Rabczuk, T., A multi-material level set-based topology optimization of flexoelectric composites, *Computer Methods in Applied Mechanics and Engineering*, 332, 2018, 47-62. <https://doi.org/10.1016/j.cma.2017.12.005>.
- [19] Guo, X., Zhang, W., Zhang, L., Robust structural topology optimization considering boundary uncertainties, *Computer Methods in Applied Mechanics and Engineering*, 253, 2013, 356-368. <http://dx.doi.org/10.1016/j.cma.2012.09.005>.
- [20] Luo, Y., Zhou, M., Wang, M.Y., Deng, Z., Reliability-based topology optimization for continuum structures with local failure constraints, *Computer and Structures*, 143, 2014, 73-84. <http://dx.doi.org/10.1016/j.compstruc.2014.07.009>.
- [21] Cheng, G., Guo, X., ϵ -relaxed approach in structural topology optimization, *Engineering Optimization*, 13, 1997, 258-266.
- [22] da Silva, G.A., Cardoso, E.L., Stress-based topology optimization of continuum structures under uncertainties, *Computer Methods in Applied Mechanics and Engineering*, 313, 2017, 647-672. <http://dx.doi.org/10.1016/j.cma.2016.09.049>.
- [23] António, C.C., Hoffbauer, L.N., Reliability-based design optimization and uncertainty quantification for optimal conditions of composite structures with nonlinear behavior, *Engineering Structures*, 153, 2017, 479-490. <http://dx.doi.org/10.1016/j.engstruct.2017.10.041>.
- [24] Chun, J., Song, J., Paulino, G.H., System reliability-based design and topology of structures under constraints on first-passage probability, *Structural Safety*, 76, 2019, 81-94. <https://doi.org/10.1016/j.strusafe.2018.06.006>.
- [25] Keshavarzadeh, V., Kirby, R.M., Narayan A., Stress-based topology optimization under uncertainty via simulation-based Gaussian process, *Computer Methods in Applied Mechanics and Engineering*, 365, 2020, 112992. <https://doi.org/10.1016/j.cma.2020.112992>.




- [26] Liu, B., Jiang, C., Li, G., Huang, X., Topology optimization of structures considering local material uncertainties in additive manufacturing, *Computer Methods in Applied Mechanics and Engineering*, 360, 2020, 112786. <https://doi.org/10.1016/j.cma.2019.112786>.
- [27] Gomez, F., Spencer, B.F., Carrion, J., Topology optimization of buildings subjected to stochastic base excitation, *Engineering Structures*, 223, 2020, 111111. <https://doi.org/10.1016/j.engstruct.2020.111111>.
- [28] Rao, S.S., *Engineering Optimization: Theory and Practice*, John Wiley and Sons, 4th Edition, 2009. <https://doi.org/10.1002/9780470549124>.
- [29] Bendsøe, M.P., Optimal shape design as a material distribution problem, *Structural Optimization*, 1989, 193-202. <https://doi.org/10.1007/BF01650949>
- [30] Le, C., Norato, J., Brums, T., Ha, C., Tortorelli, D., Stress-based topology optimization for continua, *Structural Multidisciplinary Optimization*, 41, 2010, 605-620. <https://doi.org/10.1007/s00158-009-0440-y>.
- [31] Huang, X., Xie, Y.M., *Evolutionary topology optimization of continuum structures: methods and applications*, Wiley, 2010.
- [32] Kuhinek, D., Zoriš, I., Hrženjak, P., Measurement Uncertainty in Testing of Uniaxial Compressive Strength and Deformability of Rock Samples, *Measurement Science Review*, 11, 2011, 112-117. <https://doi.org/10.2478/v10048-011-0021-2>.

ORCID iD

Rodrigo Reis Amaral  <https://orcid.org/0000-0001-9035-5806>

Julian Alves Borges  <https://orcid.org/0000-0002-0986-7634>

Herbert Martins Gomes  <https://orcid.org/0000-0001-5635-1852>



© 2022 Shahid Chamran University of Ahvaz, Ahvaz, Iran. This article is an open-access article distributed under the terms and conditions of the Creative Commons Attribution-NonCommercial 4.0 International (CC BY-NC 4.0 license) (<http://creativecommons.org/licenses/by-nc/4.0/>).

How to cite this article: Amaral R.R., Borges J.A., Gomes H.M. Proportional topology optimization under reliability-based constraints, *J. Appl. Comput. Mech.*, 8(1), 2022, 319–330. <https://doi.org/10.22055/JACM.2021.38440.3226>

Publisher's Note Shahid Chamran University of Ahvaz remains neutral with regard to jurisdictional claims in published maps and institutional affiliations.

